Finite-Size Effects of the HVP Contribution to the Muon $g-2$ with C* Boundary Conditions

2022-08-24

Sofie Martins, University of Southern Denmark
In collaboration with A. Patella, Humboldt University

Nordic Lattice Meeting, University of Helsinki

Outline

C⋆ Boundary Conditions Reduce FV Effects

[Kronfeld and Wiese 1991; Polley and Wiese 1991]

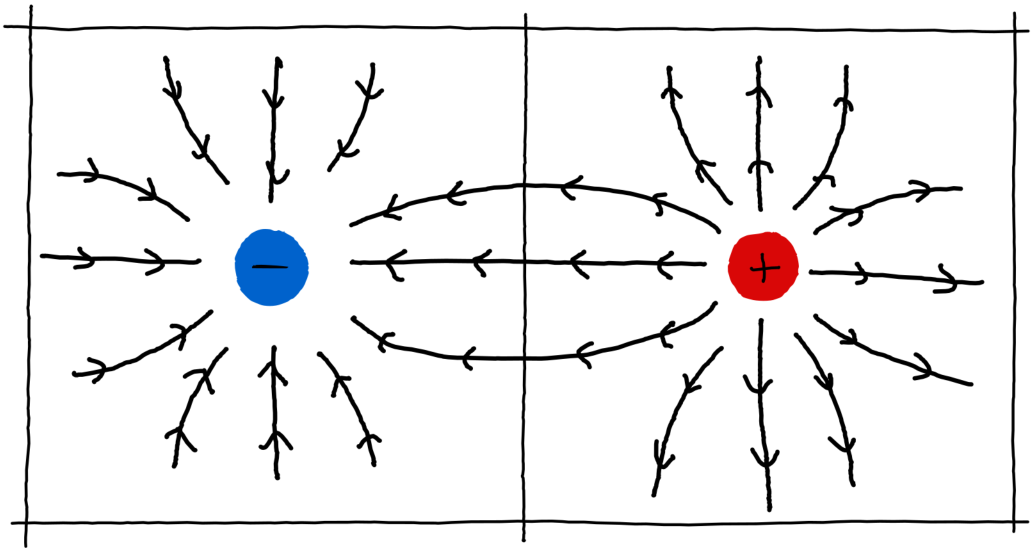

Muon g-2

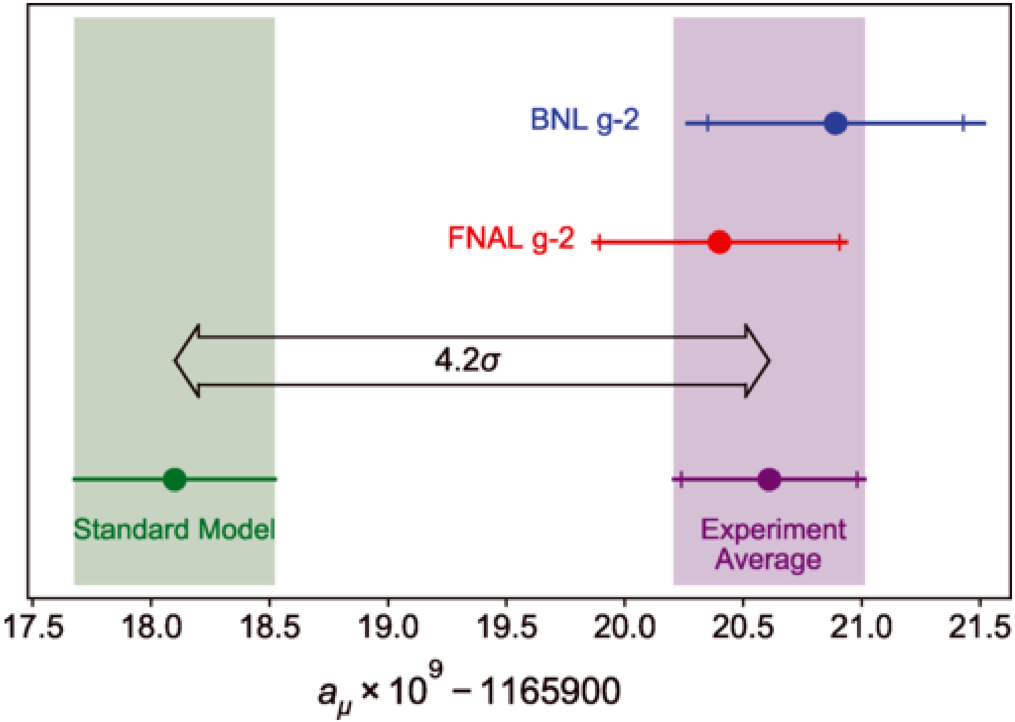

Figure: [Abi et al. 2021] $a_\mu = \frac{g-2}{2}$

HVP Contribution

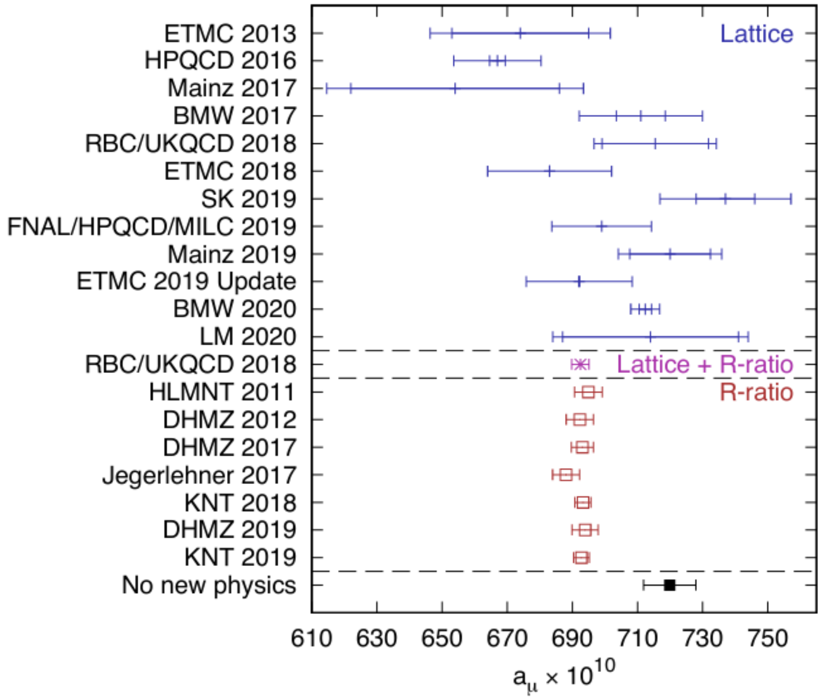

Figure: [Lehner and Meyer 2020]

Time-Window Observables

$$a_\mu^{\mathrm{LO,HVP}} = \int_0^\infty \mathrm{d}x_0 \, \mathcal{K}(x_0) G(x_0)$$

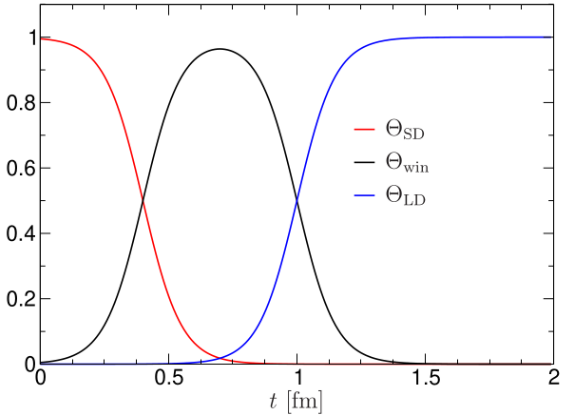

Figure: [Colangelo et al. 2022]

Time-Window Observables

continuum extrapolation

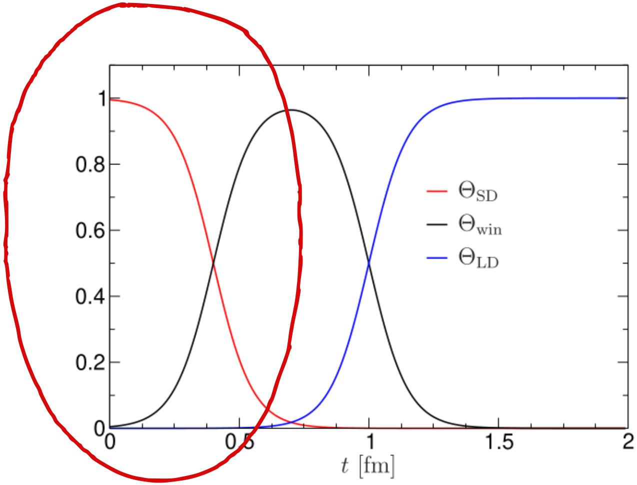

Figure: [Colangelo et al. 2022]

Time-Window Observables

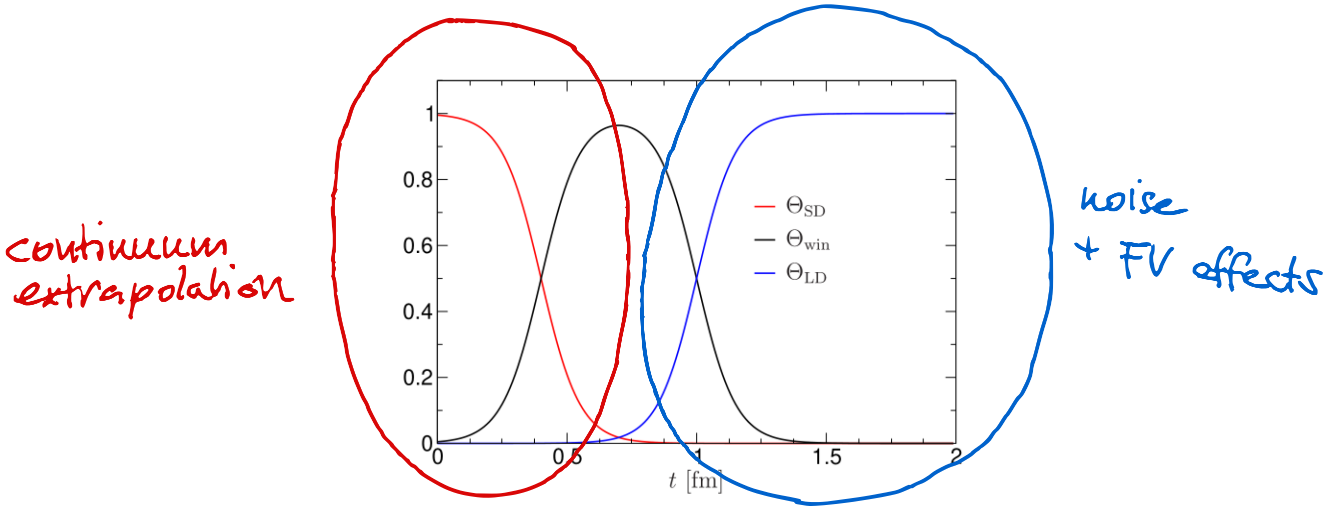

Figure: [Colangelo et al. 2022]

Time-Window Observables

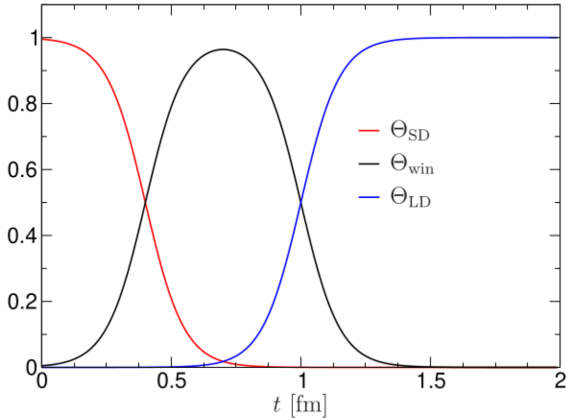

Figure: [Colangelo et al. 2022]

- Consistency checks for intermediate-time window or windows of different hadronic decay channels

C* Boundary Conditions

[Lucini et al. 2016]

$$\Psi_f(x + L\hat{\mathrm{e}}_i) = \Psi_f^{\mathrm{c}}(x) = C^{-1}\bar{\Psi}_f^{\mathrm{T}}(x)$$

$$\bar{\Psi}_f(x + L\hat{\mathrm{e}}_i) = \bar{\Psi}_f^{\mathrm{c}}(x) = -\Psi_f^{\mathrm{T}}(x)C$$

C* Boundary Conditions

[Lucini et al. 2016]

$$\Psi_f(x + L\hat{\mathrm{e}}_i) = \Psi_f^{\mathrm{c}}(x) = C^{-1}\bar{\Psi}_f^{\mathrm{T}}(x)$$

$$\bar{\Psi}_f(x + L\hat{\mathrm{e}}_i) = \bar{\Psi}_f^{\mathrm{c}}(x) = -\Psi_f^{\mathrm{T}}(x)C$$

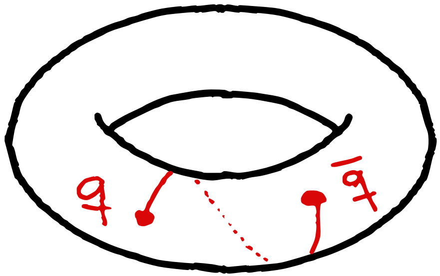

C⋆ Boundary Conditions

[Lucini et al. 2016]

$$\Psi_f(x + L\hat{\mathrm{e}}_i) = \Psi_f^{\mathrm{c}}(x) = C^{-1}\bar{\Psi}_f^{\mathrm{T}}(x)$$

$$\bar{\Psi}_f(x + L\hat{\mathrm{e}}_i) = \bar{\Psi}_f^{\mathrm{c}}(x) = -\Psi_f^{\mathrm{T}}(x)C$$

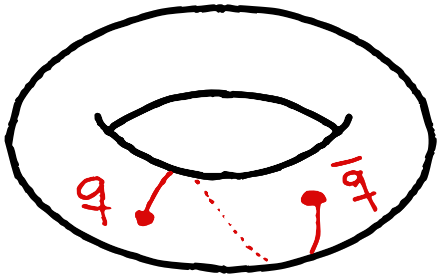

- BC violate charge & flavor conservation

C* Boundary Conditions

[Lucini et al. 2016]

$$\Psi_f(x + L\hat{\mathrm{e}}_i) = \Psi_f^{\mathrm{c}}(x) = C^{-1}\bar{\Psi}_f^{\mathrm{T}}(x)$$

$$\bar{\Psi}_f(x + L\hat{\mathrm{e}}_i) = \bar{\Psi}_f^{\mathrm{c}}(x) = -\Psi_f^{\mathrm{T}}(x)C$$

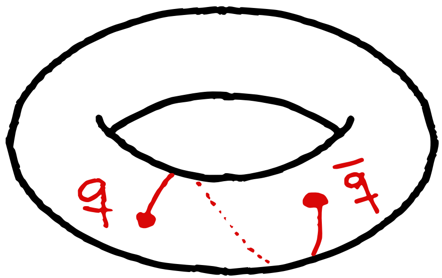

- BC violate charge & flavor conservation

$$A_\mu(x + L\hat{\mathrm{e}}_i) = A_\mu^{\mathrm{c}}(x) = -A_\mu(x)$$

Consequences from Antiperiodicity of $A_\mu(x)$

Estimator HVP (zero-momentum projection?):

$$G(x_0|T,L) = -\frac{1}{3}\int_{V_L} \langle j_k(x) j_k(0)\rangle_{T,L} \tag{1}$$

Consequences from Antiperiodicity of $A_\mu(x)$

Estimator HVP (zero-momentum projection?):

$$G(x_0|T,L) = -\frac{1}{3}\int_{V_L} \langle j_k(x) j_k(0)\rangle_{T,L} \tag{1}$$

- $j_\mu(x)$ antiperiodic

Consequences from Antiperiodicity of $A_\mu(x)$

Estimator HVP (zero-momentum projection?):

$$G(x_0|T,L) = -\frac{1}{3}\int_{V_L} \langle j_k(x) j_k(0)\rangle_{T,L} \tag{1}$$

- $j_\mu(x)$ antiperiodic
- zero-mode excluded

Consequences from Antiperiodicity of $A_\mu(x)$

Estimator HVP (zero-momentum projection?):

$$G(x_0|T,L) = -\frac{1}{3}\int_{V_L} \langle j_k(x) j_k(0)\rangle_{T,L} \tag{1}$$

- $j_\mu(x)$ antiperiodic
- zero-mode excluded
- zero-momentum projection not possible

Consequences from Antiperiodicity of $A_\mu(x)$

Estimator HVP (zero-momentum projection?):

$$G(x_0|T,L) = -\frac{1}{3}\int_{V_L} \langle j_k(x) j_k(0)\rangle_{T,L} \qquad (1)$$

- $j_\mu(x)$ antiperiodic
- zero-mode excluded
- zero-momentum projection not possible

Choose:

$$V_L = \left(-\frac{L}{2}, \frac{L}{2}\right)^3 \times (0, T) \qquad (2)$$

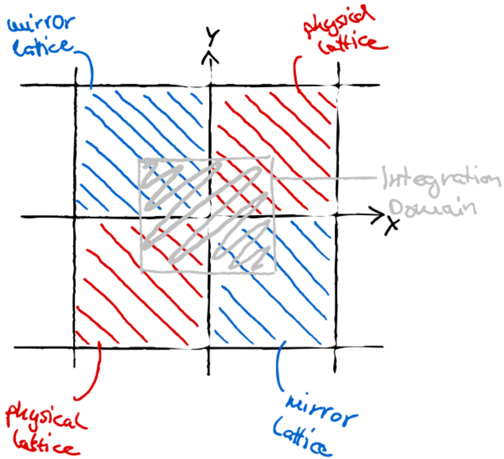

Structure of Finite-Size Effects: PBC

[Hansen and Patella 2020]

Structure of Finite-Size Effects: PBC

[Hansen and Patella 2020]

$$e^{-M_\pi L} + e^{-\sqrt{2}M_\pi L} + e^{-\sqrt{3}M_\pi L} + e^{-2M_\pi L} \dots$$

Finite-Volume Effects

Structure of Finite-Size Effects: PBC

[Hansen and Patella 2020]

$$e^{-M_\pi L} + e^{-\sqrt{2}M_\pi L} + e^{-\sqrt{3}M_\pi L} + e^{-2M_\pi L} \ldots$$

$$+e^{-M_\pi T} + \ldots + e^{-M_\pi \sqrt{L^2+T^2}} + \ldots$$

Finite-Time Effects
→ Subleading!

Structure of Finite-Size Effects: PBC

[Hansen and Patella 2020]

$$e^{-M_\pi L} + e^{-\sqrt{2}M_\pi L} + e^{-\sqrt{3}M_\pi L} + e^{-2M_\pi L} \dots$$

$$+e^{-M_\pi T} + \dots + e^{-M_\pi \sqrt{L^2+T^2}} + \dots$$

$$+e^{-M_\mathrm{K} L} + \dots$$

Higher Mass Hadrons
→ subleading

Finite-Size Effects: PBC

[Hansen and Patella 2020]

$$\Delta G_L(x_0) = -\sum_{\boldsymbol{n}\neq\boldsymbol{0}} \int \frac{\mathrm{d}p_3}{2\pi} \frac{e^{-|\boldsymbol{n}|L\sqrt{M_\pi^2+p_3^2}}}{24\pi|\boldsymbol{n}|L}$$

$$\int \frac{\mathrm{d}k_3}{2\pi} \cos(k_3 x_0) \mathrm{Re}\, T(-k_3^2, -p_3 k_3)$$

$$+\, \mathcal{O}(e^{-\sqrt{2+\sqrt{3}}M_\pi L})$$

Finite-Size Effects: PBC

[Hansen and Patella 2020]

$$\Delta G_L(x_0) = -\sum_{\boldsymbol{n}\neq\boldsymbol{0}} \int \frac{\mathrm{d}p_3}{2\pi} \frac{e^{-|\boldsymbol{n}|L\sqrt{M_\pi^2+p_3^2}}}{24\pi|\boldsymbol{n}|L}$$

$$\int \frac{\mathrm{d}k_3}{2\pi} \cos(k_3 x_0) \mathrm{Re}\, T(-k_3^2, -p_3 k_3)$$

$$+ \mathcal{O}(e^{-\sqrt{2+\sqrt{3}}M_\pi L})$$

Finite-Size Effects: PBC

[Hansen and Patella 2020]

$$\Delta G_L(x_0) = -\sum_{\boldsymbol{n}\neq\boldsymbol{0}} \int \frac{\mathrm{d}p_3}{2\pi} \frac{e^{-|\boldsymbol{n}|L\sqrt{M_\pi^2+p_3^2}}}{24\pi|\boldsymbol{n}|L}$$

$$\int \frac{\mathrm{d}k_3}{2\pi} \cos(k_3 x_0) \mathrm{Re}\, T(-k_3^2, -p_3 k_3)$$

$$+\, \mathcal{O}(e^{-\sqrt{2+\sqrt{3}}M_\pi L})$$

Finite-Size Effects: PBC

[Hansen and Patella 2020]

$$\Delta G_L(x_0) = -\sum_{\boldsymbol{n}\neq\boldsymbol{0}} \int \frac{\mathrm{d}p_3}{2\pi} \frac{e^{-|\boldsymbol{n}|L\sqrt{M_\pi^2+p_3^2}}}{24\pi|\boldsymbol{n}|L}$$

pion Compton scattering amplitude

$$\int \frac{\mathrm{d}k_3}{2\pi} \cos(k_3 x_0) \mathrm{Re}\, T(-k_3^2, -p_3 k_3)$$

$$+ \mathcal{O}(e^{-\sqrt{2+\sqrt{3}}M_\pi L})$$

Finite-Size Propagator: PBC

[Hansen and Patella 2020]

$$\Delta_{T,L}(x) = \Delta_\infty(x) + \sum_{n \in \mathbb{Z}^4 \setminus \{0\}} \Delta_\infty(x + \boldsymbol{L} n)$$

$$\boldsymbol{L} = \mathrm{diag}(T, L, L, L)$$

Finite-Size Propagator: PBC

[Hansen and Patella 2020]

$$\Delta_{T,L}(x) = \Delta_\infty(x) + \sum_{n \in \mathbb{Z}^4 \setminus \{0\}} \Delta_\infty(x + \boldsymbol{L}n)$$

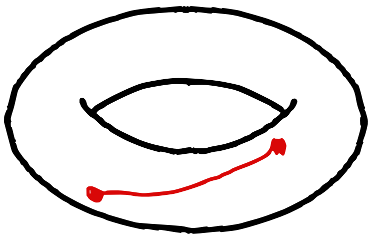

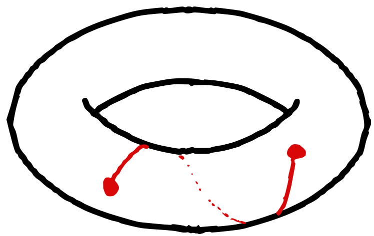

Finite-Size Propagator: PBC

[Hansen and Patella 2020]

$$\Delta_{T,L}(x) = \Delta_\infty(x) + \sum_{n \in \mathbb{Z}^4 \setminus \{0\}} \Delta_\infty(x + \boldsymbol{L}n)$$

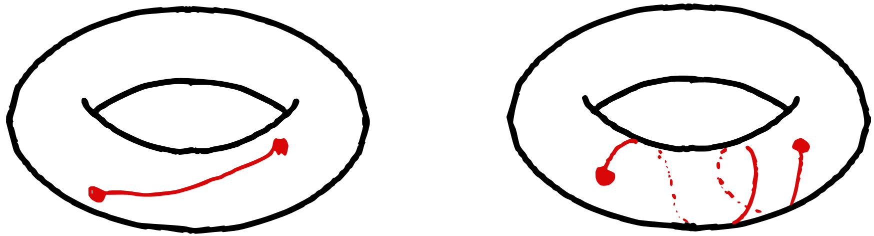

Finite-Size Propagator: PBC

[Hansen and Patella 2020]

$$\Delta_{T,L}(x) = \Delta_\infty(x) + \sum_{n \in \mathbb{Z}^4 \setminus \{0\}} \Delta_\infty(x + \boldsymbol{L}n)$$

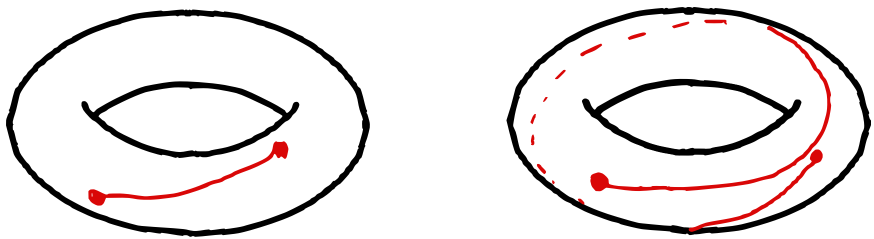

Finite-Size Propagator: PBC

[Hansen and Patella 2020]

$$\Delta_{T,L}(x) = \Delta_\infty(x) + \sum_{n \in \mathbb{Z}^4 \setminus \{0\}} \Delta_\infty(x + \boldsymbol{L} n)$$

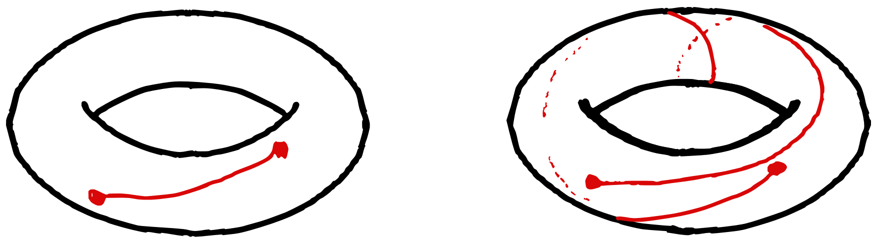

C-parity basis

$$\pi^3(x) = \pi^0(x)\,, \qquad \pi^{\pm} = \frac{\pi^1(x) \pm \mathrm{i}\pi^2(x)}{\sqrt{2}} \tag{1}$$

$$\Delta^3_{T,L}(x) = \Delta^1_{T,L}(x) = \sum_{n \in \mathbb{Z}^4} \Delta_\infty(x + \boldsymbol{L}n) \tag{2}$$

$$\Delta^2_{T,L}(x) = \sum_{n \in \mathbb{Z}^4} (-1)^{\langle \boldsymbol{n} \rangle} \Delta_\infty(x + \boldsymbol{L}n) \tag{3}$$

Finite-Size Propagator: C* BC

$$\Delta^q_{T,L}(x) = \Delta_\infty(x) + \sum_{n \in \mathbb{Z}^4 \setminus \{0\}} \frac{1 + (-1)^{q\langle \boldsymbol{n} \rangle}}{2} \Delta_\infty(x + \boldsymbol{L}n)$$

$$\langle \boldsymbol{n} \rangle = \sum_i n_i \mod 2$$

Finite-Size Propagator: C* BC

$$\Delta^{q}_{T,L}(x) = \Delta_\infty(x) + \sum_{n\in\mathbb{Z}^4\setminus\{0\}} \frac{1+(-1)^{q\langle \boldsymbol{n}\rangle}}{2}\Delta_\infty(x+\boldsymbol{L}n)$$

Finite-Size Propagator: C* BC

$$\Delta^{q}_{T,L}(x) = \Delta_\infty(x) + \sum_{n \in \mathbb{Z}^4 \setminus \{0\}} \frac{1 + (-1)^{q\langle \boldsymbol{n} \rangle}}{2} \Delta_\infty(x + \boldsymbol{L}n)$$

Finite-Size Propagator: C⋆ BC

$$\Delta^q_{T,L}(x) = \Delta_\infty(x) + \sum_{n\in\mathbb{Z}^4\setminus\{0\}} \frac{1+(-1)^{q\langle \boldsymbol{n}\rangle}}{2}\Delta_\infty(x+\boldsymbol{L}n)$$

Finite-Size Effects: C* BC

$$\Delta G_L(x_0) = -\sum_{\boldsymbol{n}\neq\boldsymbol{0}} \sum_{q=\{0,\pm 1\}} \frac{1+(-1)^{q\langle \boldsymbol{n}\rangle}}{2} \int \frac{\mathrm{d}p_3}{2\pi} \frac{e^{-|\boldsymbol{n}|L\sqrt{M_\pi^2+p_3^2}}}{24\pi|\boldsymbol{n}|L}$$

$$\int \frac{\mathrm{d}k_3}{2\pi} \cos(k_3 x_0) \mathrm{Re}\, T^q(-k_3^2, -p_3 k_3)$$

$$+\,\mathcal{O}(e^{-\sqrt{2+\sqrt{3}}M_\pi L})$$

Finite-Size Effects: C* BC

$$\Delta G_L(x_0) = -\sum_{\boldsymbol{n}\neq \boldsymbol{0}} \sum_{q=\{0,\pm 1\}} \frac{1+(-1)^{q\langle \boldsymbol{n}\rangle}}{2} \int \frac{\mathrm{d}p_3}{2\pi} \frac{e^{-|\boldsymbol{n}|L\sqrt{M_\pi^2+p_3^2}}}{24\pi|\boldsymbol{n}|L}$$

$$\int \frac{\mathrm{d}k_3}{2\pi} \cos(k_3 x_0) \mathrm{Re}\, T^q(-k_3^2, -p_3 k_3)$$

$$+\,\mathcal{O}(e^{-\sqrt{2+\sqrt{3}}M_\pi L})$$

Finite-Size Effects: C* BC

$$\Delta G_L(x_0) = -\sum_{\boldsymbol{n}\neq\boldsymbol{0}} \sum_{q=\{0,\pm1\}} \frac{1+(-1)^{q\langle \boldsymbol{n}\rangle}}{2} \int \frac{\mathrm{d}p_3}{2\pi} \frac{e^{-|\boldsymbol{n}|L\sqrt{M_\pi^2+p_3^2}}}{24\pi|\boldsymbol{n}|L}$$

$$\int \frac{\mathrm{d}k_3}{2\pi} \cos(k_3 x_0) \mathrm{Re}\, T^q(-k_3^2, -p_3 k_3)$$

$$+\,\mathcal{O}(e^{-\sqrt{2+\sqrt{3}}M_\pi L})$$

Finite-Size Effects: C* BC

$$\Delta G_L(x_0) = -\sum_{\boldsymbol{n}\neq\boldsymbol{0}} \sum_{q=\{0,\pm1\}} \frac{1+(-1)^{q\langle \boldsymbol{n}\rangle}}{2} \int \frac{\mathrm{d}p_3}{2\pi} \frac{e^{-|\boldsymbol{n}|L\sqrt{M_\pi^2+p_3^2}}}{24\pi|\boldsymbol{n}|L}$$

$$\int \frac{\mathrm{d}k_3}{2\pi} \cos(k_3 x_0) \mathrm{Re}\, T^q(-k_3^2, -p_3 k_3)$$

$$+ \mathcal{O}(e^{-\sqrt{2+\sqrt{3}}M_\pi L})$$

Finite-Size Effects: C* BC

$$\Delta G_L(x_0) = -\sum_{\boldsymbol{n}\neq\boldsymbol{0}} \sum_{q=\{0,\pm1\}} \frac{1+(-1)^{q\langle\boldsymbol{n}\rangle}}{2} \int \frac{\mathrm{d}p_3}{2\pi} \frac{e^{-|\boldsymbol{n}|L\sqrt{M_\pi^2+p_3^2}}}{24\pi|\boldsymbol{n}|L}$$

$$\int \frac{\mathrm{d}k_3}{2\pi} \cos(k_3 x_0) \mathrm{Re}\, T^q(-k_3^2, -p_3 k_3)$$

$$+\,\mathcal{O}(e^{-\sqrt{2+\sqrt{3}}M_\pi L})$$

$$\langle n \rangle = \sum_i n_i$$

Finite-Size Effects: C* BC

$$\Delta G_L(x_0) = -\sum_{\mathbf{n}\neq\mathbf{0}} \sum_{q=\{0,\pm1\}} \frac{1+(-1)^{q\langle \mathbf{n}\rangle}}{2} \int \frac{\mathrm{d}p_3}{2\pi} \frac{e^{-|\mathbf{n}|L\sqrt{M_\pi^2+p_3^2}}}{24\pi|\mathbf{n}|L}$$

$$\int \frac{\mathrm{d}k_3}{2\pi} \cos(k_3 x_0) \mathrm{Re}\, T^q(-k_3^2, -p_3 k_3)$$

$$+\,\mathcal{O}(e^{-\sqrt{2+\sqrt{3}}M_\pi L})$$

$$\langle n \rangle = \sum_i n_i$$

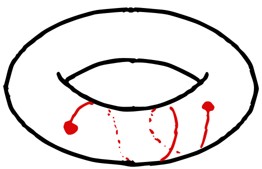

Finite-Size Effects: C⋆ BC

$$\Delta G_L(x_0) = -\sum_{\boldsymbol{n}\neq\boldsymbol{0}} \sum_{q=\{0,\pm1\}} \frac{1+(-1)^{q\langle \boldsymbol{n}\rangle}}{2} \int \frac{\mathrm{d}p_3}{2\pi} \frac{e^{-|\boldsymbol{n}|L\sqrt{M_\pi^2+p_3^2}}}{24\pi|\boldsymbol{n}|L}$$

$$\int \frac{\mathrm{d}k_3}{2\pi}\cos(k_3x_0)\,\mathrm{Re}\,T^q(-k_3^2,-p_3k_3)$$

$$+\,\mathcal{O}(e^{-\sqrt{2+\sqrt{3}}M_\pi L})$$

$\langle n\rangle = \sum_i n_i$

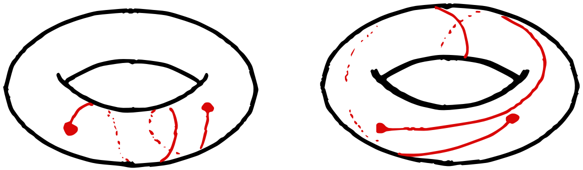

Structure of Finite-Size Effects: C* BC

$$\xcancel{e^{-M_\pi L}} + e^{-\sqrt{2}M_\pi L} + \xcancel{e^{-\sqrt{3}M_\pi L}} + e^{-2M_\pi L} \ldots$$

$$+e^{-M_\pi T} + \ldots + e^{-M_\pi \sqrt{L^2+T^2}} + \ldots$$

$$+e^{-M_\mathrm{K} L} + \ldots$$

Structure of Finite-Size Effects: C⋆ BC

$$\cancel{e^{-M_\pi L}} + e^{-\sqrt{2}M_\pi L} + \cancel{e^{-\sqrt{3}M_\pi L}} + e^{-2M_\pi L} \ldots$$

$$+e^{-M_\pi T} + \ldots + e^{-M_\pi \sqrt{L^2+T^2}} + \ldots$$

$$+e^{-M_{\mathrm{K}} L} + \ldots$$

- Charged case removed by factor $\frac{1+(-1)^{\langle \boldsymbol{n} \rangle}}{2}$

Structure of Finite-Size Effects: C* BC

$$\cancel{e^{-M_\pi L}} + e^{-\sqrt{2}M_\pi L} + \cancel{e^{-\sqrt{3}M_\pi L}} + e^{-2M_\pi L} \dots$$

$$+e^{-M_\pi T} + \dots + e^{-M_\pi \sqrt{L^2+T^2}} + \dots$$

$$+e^{-M_{\mathrm{K}} L} + \dots$$

- Charged case removed by factor $\frac{1+(-1)^{\langle \boldsymbol{n} \rangle}}{2}$
- Spectral Decomposition of T^q: Largest contribution from pole for one-pion intermediate states

Structure of Finite-Size Effects: C* BC

$$\cancel{e^{-M_\pi L}} + e^{-\sqrt{2}M_\pi L} + \cancel{e^{-\sqrt{3}M_\pi L}} + e^{-2M_\pi L} \ldots$$

$$+e^{-M_\pi T} + \ldots + e^{-M_\pi \sqrt{L^2+T^2}} + \ldots$$

$$+e^{-M_{\mathrm{K}} L} + \ldots$$

- Charged case removed by factor $\frac{1+(-1)^{\langle \boldsymbol{n} \rangle}}{2}$
- Spectral Decomposition of T^q: Largest contribution from pole for one-pion intermediate states
- Proportional to pion formfactor $\rightarrow$ zero for uncharged case, also for periodic case

FV Effects: Results

Table: $-\Delta a_\mu(L) \times 10^{10}$

$M_\pi L$	C* BC	PBC
4	9.74(1.6)	22.4(3.1)
5	3.25(0.23)	10.0(0.4)
6	1.027(0.034)	4.42(0.06)
7	0.311(0.005)	1.924(0.009)
8	0.0909(0.0008)	0.826(0.001)

Table: $-100 \times \Delta a_\mu(L)/a_\mu$

$M_\pi L$	C* BC	PBC
4	1.39	3.20
5	0.464	1.43
6	0.147	0.631
7	0.0444	0.275
8	0.0130	0.118

FV Effects: Results

Table: $-\Delta a_\mu(L) \times 10^{10}$

$M_\pi L$	C* BC	PBC
4	9.74(1.6)	22.4(3.1)
5	3.25(0.23)	10.0(0.4)
6	1.027(0.034)	4.42(0.06)
7	0.311(0.005)	1.924(0.009)
8	0.0909(0.0008)	0.826(0.001)

Table: $-100 \times \Delta a_\mu(L)/a_\mu$

$M_\pi L$	C* BC	PBC
4	1.39	3.20
5	0.464	1.43
6	0.147	0.631
7	0.0444	0.275
8	0.0130	0.118

- C* BC FV effects vanish faster than for periodic

PBC from [Hansen and Patella 2020]

Computational Cost of Precision

$C^\star$ BC $\sim$ 2.3 PBC   cost $\sim L^4$

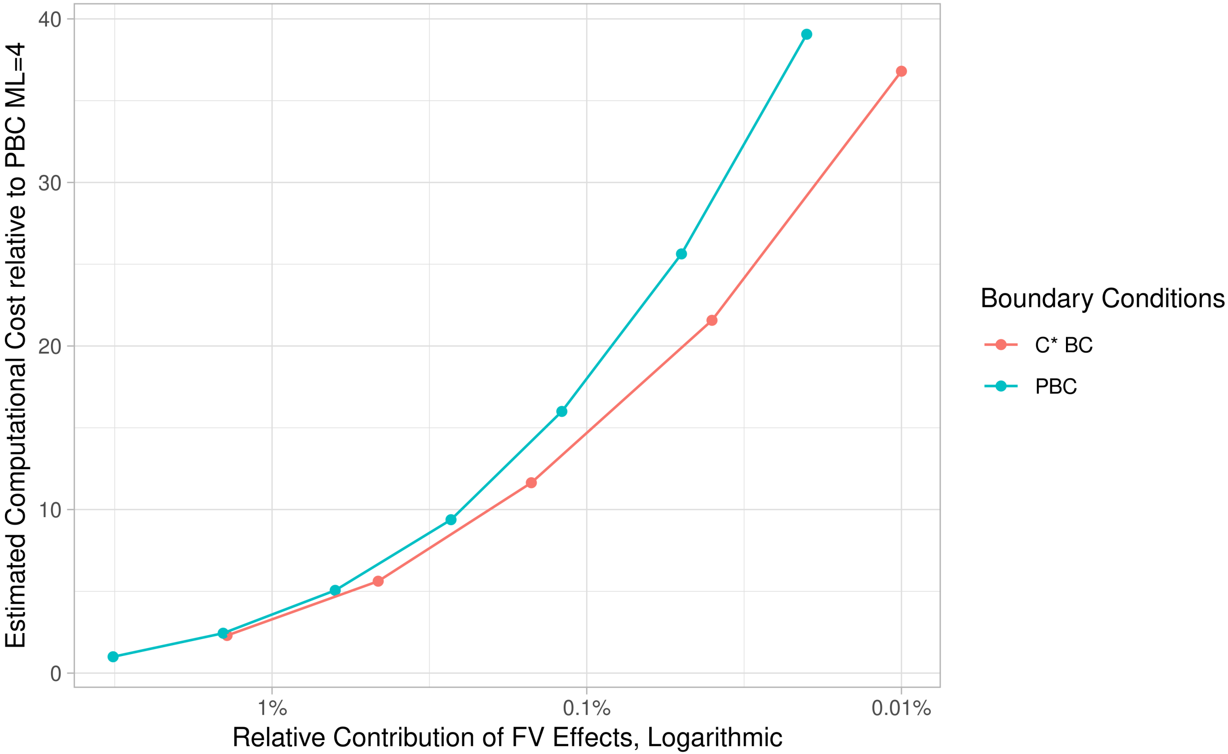

Conclusion and Related Work

- Muon $g-2$ calculations are underway

Conclusion and Related Work

- Muon $g - 2$ calculations are underway
- OpenQ*D: [Campos et al. 2020]: `https://gitlab.com/rcstar/openQxD`

Conclusion and Related Work

- Muon $g-2$ calculations are underway
- OpenQ*D: [Campos et al. 2020]:
  `https://gitlab.com/rcstar/openQxD`
- Work on FV effects of IB breaking contributions is underway

References I

Abi, B. et al. (2021). "Measurement of the Positive Muon Anomalous Magnetic Moment to 0.46 ppm". In: *Phys. Rev. Lett.* 126 (14), p. 141801. DOI: 10.1103/PhysRevLett.126.141801. URL: https://link.aps.org/doi/10.1103/PhysRevLett.126.141801.

Campos, Isabel et al. (2020). "openQ*D code: a versatile tool for QCD+QED simulations". In: *The European Physical Journal C* 80.3. ISSN: 1434-6052. DOI: 10.1140/epjc/s10052-020-7617-3. URL: http://dx.doi.org/10.1140/epjc/s10052-020-7617-3.

Colangelo, G. et al. (2022). "Data-driven evaluations of Euclidean windows to scrutinize hadronic vacuum polarization". In: *Physics Letters B*, p. 137313. DOI: 10.1016/j.physletb.2022.137313. URL: https://doi.org/10.1016%2Fj.physletb.2022.137313.

References II

Hansen, Maxwell T. and Agostino Patella (2020). "Finite-volume and thermal effects in the leading-HVP contribution to muonic ($g2$)". In: *JHEP* 10, p. 029. DOI: 10.1007/JHEP10(2020)029. arXiv: 2004.03935 [hep-lat].

Kronfeld, Andreas S. and U. J. Wiese (1991). "SU(N) gauge theories with C periodic boundary conditions. 1. Topological structure". In: *Nucl. Phys. B* 357, pp. 521–533. DOI: 10.1016/0550-3213(91)90479-H.

Lehner, Christoph and Aaron S. Meyer (2020). "Consistency of hadronic vacuum polarization between lattice QCD and the R ratio". In: *Physical Review D* 101.7. ISSN: 2470-0029. DOI: 10.1103/physrevd.101.074515. URL: http://dx.doi.org/10.1103/PhysRevD.101.074515.

References III

Lucini, Biagio et al. (2016). "Charged hadrons in local finite-volume QED+QCD with C boundary conditions". In: *JHEP* 02, p. 076. DOI: 10.1007/JHEP02(2016)076. arXiv: 1509.01636 [hep-th].

Polley, L. and U. J. Wiese (1991). "Monopole condensate and monopole mass in U(1) lattice gauge theory". In: *Nucl. Phys. B* 356, pp. 629–654. DOI: 10.1016/0550-3213(91)90380-G.

Backup

The Charged Pion Compton Scattering Amplitude

$$T^q(k^2, k\cdot p) = \mathrm{i} \lim_{\boldsymbol{p}'\to\boldsymbol{p}} \int \mathrm{d}^4x\, e^{\mathrm{i}kx}$$

$$\langle\pi^q(\boldsymbol{p}')|\, \hat{\mathrm{T}}\left\{J_\rho(x)J^\rho(0)\right\}|\pi^q(\boldsymbol{p})\rangle$$

The Charged Pion Compton Scattering Amplitude

[Hansen and Patella 2020]

$$T^q(-k_3^2, -p_3 k_3) = \lim_{p_3' \to p_3} \langle \pi^q(p_3' \hat{e}_3) | \, J_\rho(0) \hat{\mathrm{O}} J^\rho(0) \, | \pi^q(p_3 \hat{e}_3) \rangle$$

$$\hat{\mathrm{O}} = \frac{(2\pi)^3 \delta(\hat{\mathrm{P}}_1)\delta(\hat{\mathrm{P}}_2)\delta(\hat{\mathrm{P}}_3 - p_3 - k_3)}{\hat{\mathrm{H}} - \sqrt{\hat{\mathrm{p}}_3^2 + M_\pi^2} - \mathrm{i}\varepsilon}$$

The Charged Pion Compton Scattering Amplitude

[Hansen and Patella 2020]

$$T^q(-k_3^2, -p_3 k_3) = \lim_{p_3' \to p_3} \langle \pi^q(p_3' \hat{e}_3) | \, J_\rho(0) \hat{\mathrm{O}} J^\rho(0) \, | \pi^q(p_3 \hat{e}_3) \rangle$$

$$\hat{\mathrm{O}} = \frac{(2\pi)^3 \delta(\hat{\mathrm{P}}_1)\delta(\hat{\mathrm{P}}_2)\delta(\hat{\mathrm{P}}_3 - p_3 - k_3)}{\hat{\mathrm{H}} - \sqrt{\hat{\mathrm{p}}_3^2 + M_\pi^2} - \mathrm{i}\varepsilon}$$

Decomposition

[Hansen and Patella 2020]

$$\mathbb{1} = |\Omega\rangle\langle\Omega|$$

$$+ \sum_{q=\{0,\pm 1\}} \int \frac{\mathrm{d}^3\ell}{(2\pi)^3} \frac{1}{2E(\ell)} |\pi^q(\boldsymbol{\ell})\rangle\langle\pi^q(\boldsymbol{\ell})|$$

$$+ \theta(\hat{\mathrm{M}} - 2M_\pi)$$

Decomposition

[Hansen and Patella 2020]

$$\mathbb{1} = |\Omega\rangle \langle\Omega|$$

– vacuum contribution

$$+ \sum_{q=\{0,\pm 1\}} \int \frac{\mathrm{d}^3\ell}{(2\pi)^3} \frac{1}{2E(\ell)} |\pi^q(\boldsymbol{\ell})\rangle \langle\pi^q(\boldsymbol{\ell})|$$

$$+ \theta(\hat{\mathrm{M}} - 2M_\pi)$$

Decomposition

[Hansen and Patella 2020]

$$\mathbb{1} = |\Omega\rangle\langle\Omega|$$

$$+ \sum_{q=\{0,\pm 1\}} \int \frac{\mathrm{d}^3\ell}{(2\pi)^3} \frac{1}{2E(\ell)} |\pi^q(\boldsymbol{\ell})\rangle\langle\pi^q(\boldsymbol{\ell})|$$

one-pion contribution

$$+ \theta(\hat{\mathrm{M}} - 2M_\pi)$$

Decomposition

[Hansen and Patella 2020]

$$\mathbb{1} = |\Omega\rangle\langle\Omega|$$

$$+ \sum_{q=\{0,\pm 1\}} \int \frac{\mathrm{d}^3\ell}{(2\pi)^3} \frac{1}{2E(\ell)} |\pi^q(\boldsymbol{\ell})\rangle\langle\pi^q(\boldsymbol{\ell})|$$

$$+ \theta(\hat{\mathrm{M}} - 2M_\pi)$$ — multi-particle & higher mass

Decomposition

$$T^q = T^q_{\mathrm{vac}} + T^q_{1\pi} + T^q_{\mathrm{MP}}$$

Decomposition

$$T^q = T^q_{\text{vac}} + T^q_{1\pi} + T^q_{\text{MP}}$$

Vacuum Contribution

$$T^q_{\text{vac}} \propto \langle \pi^q | \, J_\mu \, | \Omega \rangle = 0$$

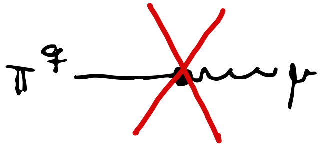

Decomposition

$$T^q = T^q_{\text{vac}} + T^q_{1\pi} + T^q_{\text{MP}}$$

Vacuum Contribution

$$T^q_{\text{vac}} \propto \langle \pi^q | J_\mu | \Omega \rangle = 0$$

One-Pion Contribution

$$T^q_{1\pi} = T^q_{1\pi,\text{pole}} + T^q_{1\pi,\text{reg}}$$

Decomposition

$$T^q = T^q_{\mathrm{vac}} + T^q_{1\pi} + T^q_{\mathrm{MP}}$$

Vacuum Contribution

$$T^q_{\mathrm{vac}} \propto \langle \pi^q | J_\mu | \Omega \rangle = 0$$

One-Pion Contribution

$$T^q_{1\pi} = T^q_{1\pi,\mathrm{pole}} + T^q_{1\pi,\mathrm{reg}}$$

$$\boxed{\Rightarrow T^q = T^q_{\mathrm{pole}} + T^q_{\mathrm{reg}}}$$

Decomposition

$$T^q = T^q_{\text{vac}} + T^q_{1\pi} + T^q_{\text{MP}}$$

Vacuum Contribution

$$T^q_{\text{vac}} \propto \langle \pi^q | \, J_\mu \, | \Omega \rangle = 0$$

One-Pion Contribution

$$T^q_{1\pi} = T^q_{1\pi,\text{pole}} + T^q_{1\pi,\text{reg}}$$

+ T_{rep} → χPT

$$\boxed{\Rightarrow T^q = T^q_{\text{pole}} + T^q_{\text{reg}}}$$

→ small

The Pole Contribution is Zero for Uneven Numbers of Translations

Charged Case

$$\frac{1 + (-1)^{q\langle \boldsymbol{n} \rangle}}{2}$$

The Pole Contribution is Zero for Uneven Numbers of Translations

Charged Case

$$\frac{1+(-1)^{q\langle \boldsymbol{n} \rangle}}{2}$$

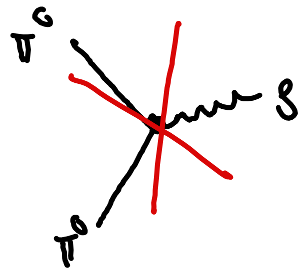

Uncharged Case

$$T^0_{1\pi,\mathrm{pole}} \propto |\, \langle \pi^0(\boldsymbol{\ell}')|\, J_\rho(0)\, |\pi^0(\boldsymbol{\ell})\rangle\, |^2 = 0$$

Pole Contribution

Table: $-100 \times \frac{\Delta a(L)}{a_\mu}$

$M_\pi L$	$\lvert \boldsymbol{n} \rvert = \sqrt{2}$	2	$\sqrt{6}$	$2\sqrt{2}$	Sum	PBC
4	1.16	0.104	0.0944	0.0128	1.38	3.17
5	0.428	0.0199	0.0112	0.00103	0.461	1.42
6	0.141	0.00349	0.00124	0.0000764	0.146	0.630
7	0.0433	0.000582	0.000130	$< 10^{-5}$	0.0440	0.274
8	0.0128	0.0000936	0.0000132	$< 10^{-5}$	0.0129	0.118

PBC from [Hansen and Patella 2020]

All-orders Expansion in EFT

[Hansen and Patella 2020]

$G(x_0) =$